Probing Cluster Transfer in Peripheral Collisions of ^{40}Ar on ^{64}Ni at 15 MeV/nucleon

Chrysi Giannitsa[1,*], *Georgios* Souliotis[1], *Theo* Depastas[2], *Stergios* Koulouris[1], *Konstantinos* Gkatzogias[1], *Martin* Veselsky[3], *Sherry* Yennello[2], and *Aldo* Bonasera[2]

[1]Laboratory of Physical Chemistry, Department of Chemistry, National and Kapodistrian University of Athens, Athens, Greece
[2]Cyclotron Institute, Texas A&M University, College Station, Texas, USA
[3]Institute of Experimental and Applied Physics, Czech Technical University, Prague, Czech Republic

Abstract. This work focuses on the study of the yields and momentum distributions of projectile-like fragments from ^{40}Ar collisions with target ^{64}Ni at 15 MeV/nucleon, using experimental data obtained in previous work with the MARS spectrometer at the Cyclotron Institute at Texas A&M University. Motivated by the current activity on clustering, we focused our attention on the channel corresponding to the production of the ^{36}S ejectile, which may have resulted from the removal of an alpha particle cluster from the ^{40}Ar projectile. The experimental distributions were compared with two dynamical models, the deep-inelastic transfer (DIT) model and the constrained molecular dynamics (CoMD) model, followed by the de-excitation code GEMINI. The observed discrepancies potentially indicate direct cluster transfer in quasi-elastic peripheral collisions. By comparing our experimental data with appropriate models, we hope to gain valuable insight into the mechanisms governing clustering and cluster transfer in peripheral collisions in the Fermi energy regime.

1 Introduction

Nucleonic matter behaves as a homogeneous quantum liquid (Fermi liquid) [1]. However, finite nuclei behave transiently as clusters of protons and neutrons. Currently, there is renewed interest in cluster effects, from both experimental and theoretical perspectives [2]. Cluster structures can be observed when the excitation energy is close to the corresponding decay threshold [1, 3].

Considering these observations, we expect that peripheral heavy ion collisions may provide optimal conditions for cluster formation and may favour the possibility of cluster transfer. Accordingly, we attempted to examine possible direct cluster transfer in the reaction ^{40}Ar (15 MeV/nucleon) + ^{64}Ni. Mass and momentum distributions of ejectiles from the above reaction were detected employing the MARS recoil separator at the Cyclotron Institute at Texas A&M University [5]. The experimental data were compared with the theoretical calculations adopting two dynamical models namely, the Deep Inelastic Transfer (DIT) [8] and the Constrained Molecular Dynamics (CoMD) [9], each one coupled to the statistical de-excitation code GEMINI [6]. The model calculations offer an adequate description of mass distributions. Focusing on momentum distributions of ^{36}S ejectiles, we obtain evidence for possible cluster transfer mechanisms that may contribute to ^{36}S production.

The present article is organized as follows: In Section 2, a description of the experimental setup and measurements is presented. In Section 3, the theoretical framework of the model is described. In Section 4, we discuss the comparisons of the experimental distributions with theoretical calculations. Finally, in Section 5, a discussion and conclusions are provided.

2 Experimental Details

The experimental data that we used in this work were obtained in previous work with the MARS recoil separator of the Cyclotron Institute at Texas A&M University. With this experimental setup, the projectile-like fragments of the ^{40}Ar + ^{64}Ni reaction at 15 MeV/nucleon were collected and identified [5]. An $^{40}Ar^{9+}$ (15 MeV/nucleon) beam, accelerated by the K500 Cyclotron, interacted with a ^{64}Ni target with thickness of 2 mg/cm^2. The beam was set at a 4° angle, with respect to the optical axis of the separator and the products were collected in a polar angular range $\Delta\theta$ = 2.2°-5.8° in a solid angle window of $\Delta\Omega$ = 4 msr. The fragments, after the interaction with the target, passed through a parallel-plate avalanche counter (PPAC) located at the dispersive image of MARS, which provided the position and the magnetic rigidity of the products as well as their START time. Subsequently, the projectile-like fragments were focused at the end of the separator passing through a second PPAC (for STOP-time information) and were collected in a ΔE-E Si detector telescope. The particle identification procedure was based on standard techniques of magnetic rigidity, energy-loss, residual energy and time-of-flight on an event-by-event basis, as described in detail in [4, 5]. Data were obtained in the

*e-mail: chryssigiann@chem.uoa.gr

range of magnetic rigidity settings from 1.1-1.5 Tm, sufficient to cover the neutron rich nuclides, which was the focus of the experimental measurement [5, 6].

3 Brief Overview of Theoretical Framework

The calculations performed are based on a two-step Monte Carlo approach. The dynamical phase of the interaction was simulated using two theoretical frameworks: the DIT model and the CoMD model.

The Deep-Inelastic Transfer (DIT) model [8] is a phenomenological model, used in peripheral collisions in the Fermi energy region. Assuming initially that both the projectile and the target are spherical entities, they approach each other along Coulomb trajectories. When the dinuclear system falls within the range of nuclear interaction, it is depicted as two Fermi gases in contact, allowing a stochastic nucleon exchange through a "window" that opens between the touching nuclear surfaces.

The Constrained Molecular Dynamics (CoMD) model [9], a microscopic code based on the framework of quantum molecular dynamics (QMD), assumes that nucleons are localized Gaussian wavepackets and the interaction among them is a Skyrme-type potential. In this model, the Pauli exclusion principle is enforced through a constraint on phase space at each step of the calculation. The requirements for the phase space occupation $\overline{f}_i$ is:

$$\overline{f}_i \leq 1$$

$$\overline{f}_i = \sum \delta_{\tau i}\delta_{\tau j}\delta_{si}\delta_{sj} \int f_j(r,p)d^3rd^3p \qquad (1)$$

where $f_i(\overrightarrow{r},\overrightarrow{p})$ is the nucleon phase space occupation function and s_i and τ_i the z component of spin and isospin, respectively. The integration is performed in a hypercube of volume h^3 in the phase space. The occupation fraction is scaled empirically in the model as

$$\overline{f}_i \rightarrow \frac{128}{paulm}\overline{f}_i \qquad (2)$$

For the CoMD calculations we used optimized ground state configurations and parameters as reported in [6]. We call these calculations as “standard”. Furthermore, motivated by recent work [10] on the crucial role of the Pauli principle in the clustering phenomenon, we attempted to enhance the Pauli constraint (phase space constraint, eq. 1, 2) by lowering the value of paulm. We will call this calculation the “enhanced Pauli constraint” calculation. More specifically, in some of our calculations, we have enhanced the the Pauli principle by lowering the standard value of paulm=87 to paulm=80.

The standard value of nuclear matter compressibility used in our calculations is K=254 MeV. Furthermore, we used two additional values K=200 and 308 MeV. We remind that the compressibility of nuclear matter represents the susceptibility of the nucleus to compression and is the second derivative of energy with respect to density, as shown in the eq. (3):

$$K = 9{\rho_0}^2 \frac{\partial^2}{\partial\rho^2}\left(\frac{E}{A}\right) \qquad (3)$$

From the recent work of our group [6, 7] we have gained confidence that the above two models can reasonably well describe the mechanism of nucleon exchange, as a sequential transfer of nucleons. In addition, however, the CoMD model, because of its microscopic many-body approach, may inherently lead to some clusterization, a feature that has to be further investigated and developed. Furthermore, we intend to explore the possibility of direct transfer of a cluster from a projectile to a target and vice versa, or cluster breakup from the projectile. These possibilities are schematically depicted in Figure 1.

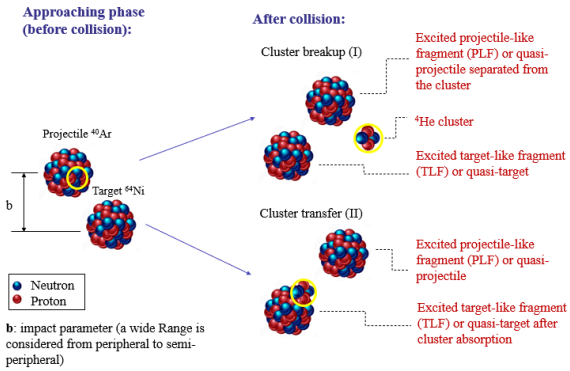

Figure 1. Schematic representation of the mechanisms of (I) direct cluster breakup of the projectile and (II) direct cluster transfer from the projectile to the target in a peripheral collision.

After the dynamical phase of the reaction, the deexcitation of the primary fragments was described using the GEMINI statistical deexcitation code [6]. In our discussion, we will refer to the combined DIT/GEMINI calculations simply as DIT calculations and, similarly, to the CoMD/GEMINI ones as CoMD calculations.

4 Experimental results and comparison with model calculations

In this section, we compare the calculations performed with the DIT and CoMD models with the experimental data. We present results of projectile-like fragments for the reaction between ^{40}Ar and ^{64}Ni, which may have resulted from alpha-particle cluster pick-up or removal.

For the DIT model, standard parameters were used as in our previous works. For the CoMD calculations we will show the standard, the enhanced Pauli, as well as the K=200 and K=308 calculations. We note that the theoretical distributions were filtered taking into account the Bρ range of the experiment and the polar (horizontal) angular window $\Delta\theta = 2.2°$–$5.8°$ of the MARS separator.

Before we continue our discussion on the p/A distributions, we present measured mass distributions of selected projectile fragments with Z=18–15 from the ^{40}Ar (15 MeV/nucleon) + ^{64}Ni reaction in Figure 2. We note that the measured distributions in the solid angle window of $\Delta\Omega$=4 msr were integrated over the azimuthal angle, which corresponds to multiplying the measured data by a factor of 7. Thus, we derived the production cross section for each isotope in the polar angular interval $\Delta\theta$=2.2°-5.8°.

In the mass distributions shown in Figure 2, we observe that the theoretical calculations lead to cross sections that are in overall reasonable agreement with the experimental data. The neutron-rich as well as the neutron-deficient sides of the distributions are rather well described by both theoretical models, as the calculations have been properly filtered, regarding both angular range and magnetic rigidity. The orange arrow in panel (c) indicates the isotope ^{36}S, produced with large cross section. We assume that it may have been produced in part by the ^{4}He cluster breakup or transfer from the ^{40}Ar projectile.

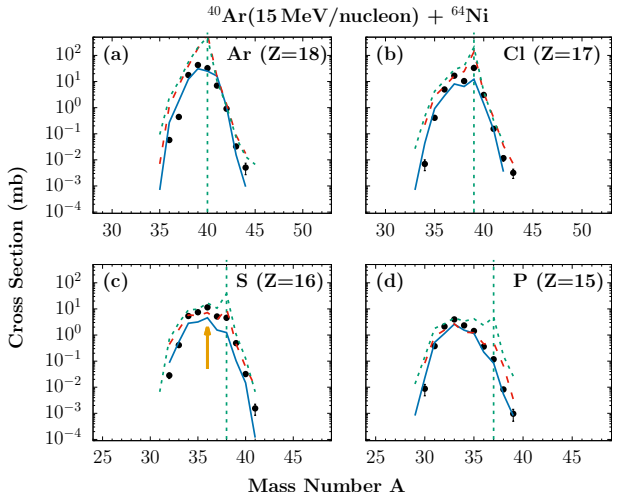

Figure 2. Selected projectile fragment mass distributions for the ^{40}Ar (15 MeV/nucleon) reaction with ^{64}Ni for elements with Z = 15-18. Black circles: experimental data. Solid (blue) line: DIT calculation. Dashed (red) line: standard CoMD calculation. Dotted (green) line: CoMD calculation with enhanced Pauli constraint. The vertical (green) dashed line the starting point of neutron pickup. The orange arrow in the panel (c) indicates ^{36}S, assumed to have been produced in part by a direct cluster breakup of the ^{40}Ar projectile.

In our subsequent analysis (Figures 3-5, below), we present the measured differential cross sections with respect to the linear momentum per nucleon (p/A) of the fragments instead of the kinetic energy. The momentum per nucleon represents the velocity of the ejectiles and allows a direct comparison with the velocity of the beam. Furthermore, similarly to the kinetic energy, it constitutes a good measure of the energy dissipation and can provide important information on the reaction mechanism.

In addition, we note that the experimental data have pronounced "dips"; one pronounced dip at 150 MeV/c and one at 160 MeV/c. These dips are the result of software gates imposed during the data analysis to remove the elastically scattered beam.

In the channel we are studying, the (green) vertical dashed line indicates the velocity of the projectile. We could consider that the momentum distribution is qualitatively divided into two energy regions: on the right side of the (yellow) vertical solid line, we discern an apparent peak (a "band") near the beam velocity (quasi-elastic region), while on the left side of the (yellow) vertical solid line we observe an extended region of higher excitation energies of the dinuclear system, corresponding to more dissipative events. Our investigation focuses on the quasi-elastic part of the distribution, as clustering is favoured at lower energies, close to the corresponding decay threshold.

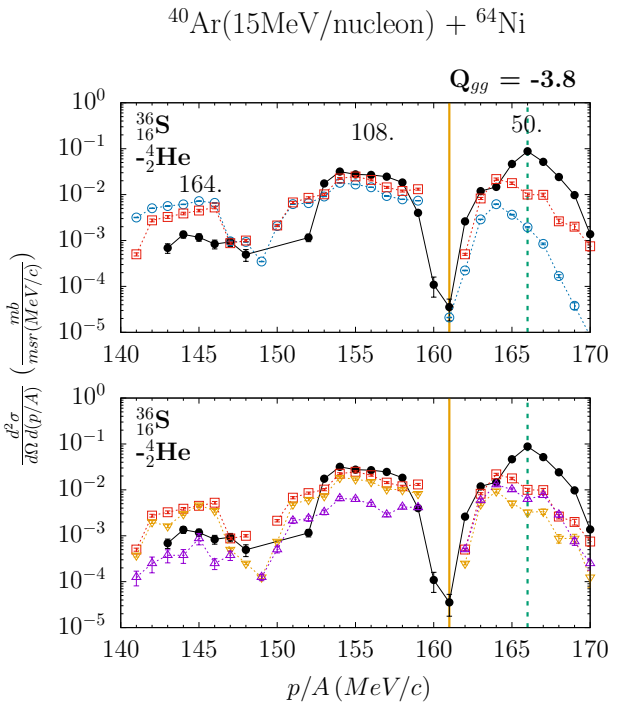

Figure 3. Momentum distribution of ^{36}S projectile fragment for the ^{40}Ar (15 MeV/nucleon) reaction with ^{64}Ni. Black points: experimental data. Circles (blue): standard DIT calculation, squares (red): standard CoMD calculation. Inverted triangles (yellow): CoMD calculation involving nucleon transfer. Triangles (purple): CoMD calculation involving nucleon breakup. The (green) vertical dashed line shows the velocity of the projectile, the vertical solid (yellow) line shows a qualitative separation of the energy regions. The numbers above some peaks give the total excitation energy (in MeV) obtained from binary kinematics using the corresponding p/A values.

In Figure 3 we present the experimental data for the momentum distribution of the ^{36}S fragment. We focused our interest on this fragment because it has a large production cross-section and may have an increased probability

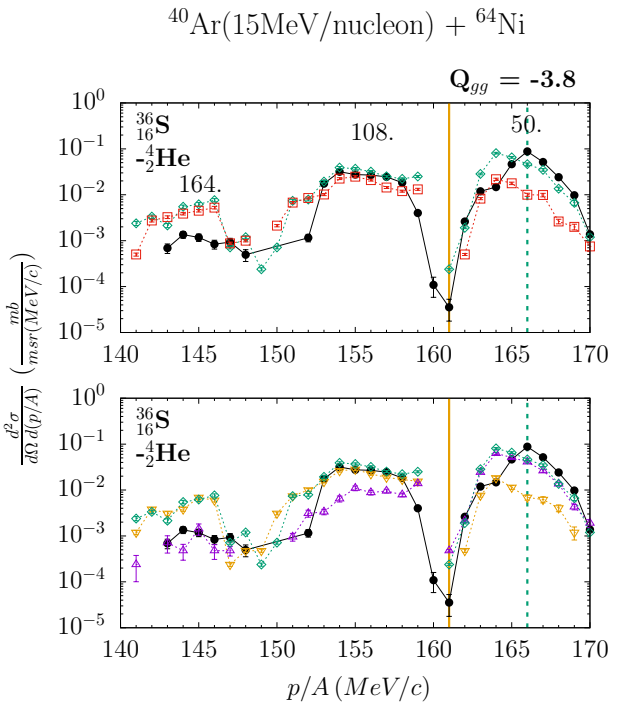

Figure 4. Momentum distributions of ^{36}S projectile fragment from the ^{40}Ar (15 MeV/nucleon) reaction with target ^{64}Ni, with enhanced Pauli constraint (paulm=80). Black points: experimental data. Circles (blue): standard DIT calculation. Squares (red): CoMD calculation (paulm=87). Diamonds (green): CoMD calculation with enhanced Pauli constraint (paulm=80). Inverted triangles (yellow): CoMD calculation with paulm=80 involving nucleon transfer. Triangles (purple): CoMD calculation with paulm=80 involving nucleon breakup.

of having been formed by a ^{4}He cluster breakup from the ^{40}Ar projectile. The part of the distribution that we are interested in is the quasi-elastic one, located at the right part of the distribution, as mentioned previously.

The calculations with DIT are obviously lower than those with CoMD. The CoMD calculations appear to better describe the experimental data, but still underestimate them. It is obvious that in the right part of the momentum distribution there is a discrepancy between the experimental data and the calculations. This may indicate the presence of a mechanism beyond nucleon exchange that is rather adequately described by DIT and, also, CoMD. Consequently, we may assume the contribution of a ^{4}He cluster breakup and/or transfer from the ^{40}Ar projectile that cannot be described by either the DIT or the CoMD model.

At this point, we have devided the CoMD calculations in two parts: the transfer part, where we assume that nucleons are transferred from the projectile to the target, and the breakup part, that we assume that the nucleons are emitted from the projectile (breakup). In the plot of CoMD calculations describing breakup and transfer we can make a general observation: the nucleon transfer from the projectile to the target is favored in the dissipative part of the distribution, while the breakup from the projectile seems to be favored in the quasi-elastic part of the distribution, where lower total excitation energies for the dinuclear projectile-target system dominate.

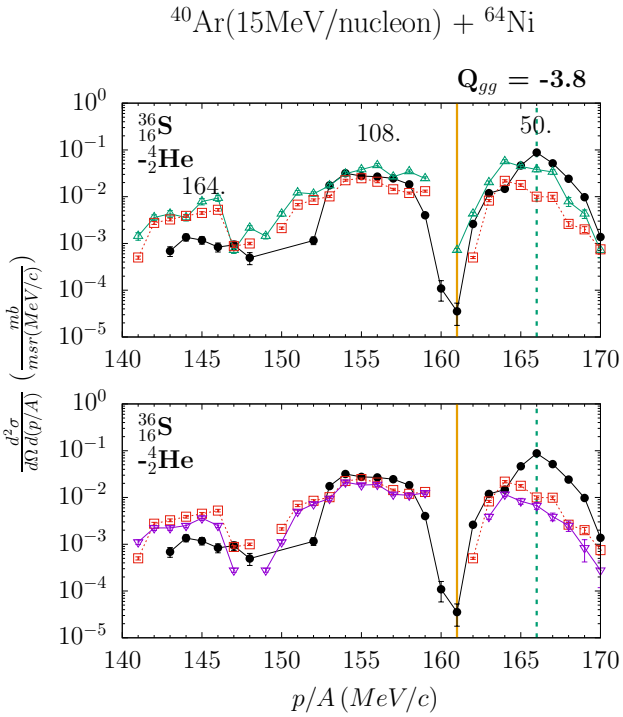

Figure 5. Momentum distributions of the ^{36}S projectile fragment from the ^{40}Ar (15 MeV/nucleon) reaction with target ^{64}Ni. Experimental data: solid black points. Triangles (green): CoMD calculation with K=200. Squares (red): CoMD calculation with K=254. Inverted triangles (purple): CoMD calculation with K=308. As in the previous figures, the numbers above some peaks give the total excitation energy (in MeV) obtained from the binary kinematics using the corresponding p/A values.

Figure 4 shows again the experimental data for the momentum distribution of the ^{36}S fragment, along with the CoMD calculations, where we applied enforcement of the Pauli principle by reducing the value of the parameter paulm from 87 to 80. The CoMD calculations with paulm=80 better describe the experimental data, especially in the quasi-elastic part of the distribution. This is an important observation pointing to the crucial role of the Pauli principle in the process of clustering and cluster transfer.

In Figure 5, we show the effect of compressibility on the CoMD calculated momentum distributions compared to the experimental data for the ^{36}S fragment. So far, for the standard CoMD calculations we use the compressibility K=254 MeV (red). Furthermore, we show calculations with K=200 MeV (green triangles) and K=308 MeV (purple inverted triangles). The CoMD calculation with K=200 is higher than the standard one, while the calculation with K=308 is slightly lower. It is interesting to note

that the calculation with K=200 appears to have an effect similar to that of the enhanced Pauli calculation.

Further on, using the primary results of the CoMD calculations, we attempted to count the alpha-particles ejected during the reaction and the projectile-like and target-like nuclei that may have resulted from alpha particle pickup or removal (breakup). While, this work is in progress, our initial observations indicate that the enhanced Pauli calculation implies enhanced clustering and cluster transfer. Similar behaviour is noticed in the calculation with K=200, whereas the standard calculation (paulm=87) and the calculation with K=308 appear to favour independent nucleon breakup or transfer rather than clustering [11].

5 Summary and Conclusions

The present work focuses on the study of fragments that may have been formed by cluster removal or transfer in peripheral collisions in the Fermi energy regime. We presented the mass and momentum distributions of projectile-like fragments from the reaction of a ^{40}Ar beam at 15 MeV/nucleon with ^{64}Ni target. In addition, we compared the experimental distributions with calculations using the theoretical models DIT and CoMD, followed by the GEMINI de-excitation code.

We tried to vary the parameters of the CoMD model in order to improve its ability to describe the experimental momentum distributions. In this work, we found that an enhancement of the Pauli constraint has a significant effect on the calculated distributions. Moreover, we studied the effect of the nuclear matter compressibility on the CoMD calculations. In our study we particularly focused on the quasi-elastic part of the momentum distribution, as the corresponding low excitation energies of the system provide suitable conditions for cluster formation and, thus, breakup or transfer. Further detailed investigation and possible improvements of the CoMD model may be required to adequately describe the experimental data and gain insight into the mechanism of clustering and cluster transfer.

References

[1] J.-P. Ebran, E. Khan, T. Niksic and D. Vretenar, How atomic nuclei cluster. Nature, **487**, 341 (2012). https://doi.org/10.1038/nature11246

[2] J. Tanaka, Z. Yang, S. Typel et al., Formation of α clusters in dilute neutron-rich matter. Science **371**, 6526, 260 (2021). https://www.science.org/doi/10.1126/science.abe4688

[3] M. Freer, The clustered nucleus—cluster structures in stable and unstable nuclei. Rep. Prog. Phys., **70**, 2149 (2007). http://dx.doi.org/10.1088/0034-4885/70/12/R03

[4] G. A. Souliotis, M. Veselsky, S. Galanopoulos et al., Approaching neutron-rich nuclei toward the r-process path in peripheral heavy-ion collisions at 15 MeV/nucleon. Phys. Rev. C, 84, 064607 (2011). https://doi.org/10.1103/PhysRevC.84.064607

[5] A. Papageorgiou, G. A. Souliotis, K. Tshoo et al., Neutron-rich rare isotope production with stable and radioactive beams in the mass range A ~40–60 at beam energy around 15 MeV/nucleon. J. Phys. G: Nucl. Part. Phys., **45**, 095105 (2018). https://dx.doi.org/10.1088/1361-6471/aad7df

[6] K. Palli, G. A. Souliotis, T. Depastas et al., Microscopic dynamical description of multinucleon transfer in 40Ar induced peripheral collisions at 15 MeV/nucleon, EPJ Web Conf., **252**, 07002 (2021). https://doi.org/10.1051/epjconf/202125207002

[7] S. Koulouris, G.A. Souliotis, F. Cappuzzello et al., Multinucleon transfer channels from 70Zn (15 MeV/nucleon) + 64Ni collisions. Phys. Rev. C, **108**, 044612 (2023). https://doi.org/10.1103/PhysRevC.108.044612

[8] L. Tassan-Got and C. Stephan, Deep inelastic transfers: A way to dissipate energy and angular momentum for reactions in the Fermi energy domain. Nucl. Phys. A, **524**, 121 (1991). https://doi.org/10.1016/0375-9474(91)90019-3

[9] M. Papa, T. Maruyama and A. Bonasera, Constrained molecular dynamics approach to fermionic systems. Phys. Rev. C, **64**, 024612 (2001). https://doi.org/10.1103/PhysRevC.64.024612

[10] S. Ohkubo, Luneburg-lens-like universal structural Pauli attraction in nucleus-nucleus interactions : Origin of emergence of cluster structures and nuclear rainbows. Phys. Rev. C, **93**, 041303 (2014). https://doi.org/10.1103/PhysRevC.93.041303

[11] Ch. Giannitsa, Investigating Clustering and Cluster Transfer in Peripheral Collisions of ^{40}Ar on ^{64}Ni at 15 MeV/nucleon. MSc Dissertation (in preparation), Laboratory of Physical Chemistry, Department of Chemistry, National and Kapodistrian University of Athens, Athens, Greece (2024).